The Hubbard model at intermediate coupling: renormalization of the interaction strength

1998 J. Phys.: Condens. Matter 10 2915

(http://iopscience.iop.org/0953-8984/10/13/010)

J. Phys.: Condens. Matter **10** (1998) 2915–2932. Printed in the UK PII: S0953-8984(98)89650-1

The Hubbard model at intermediate coupling: renormalization of the interaction strength

V Janiš

Institute of Physics, Academy of Sciences of the Czech Republic, Na Slovance 2, CZ-18040 Praha 8, Czech Republic

Received 1 December 1997

Abstract. We analyse the behaviour of correlated electrons described by Hubbard-like models at intermediate coupling. We argue that with increasing interaction a pole in a generic two-particle Green function is approached. The pole signals condensation of electron–hole pairs and a metal–insulator transition at half-filling. The two-particle singularity calls for a sophisticated renormalization of the interaction strength. A self-consistent diagrammatic technique with renormalized two-particle Green functions is developed. The theory is based on a linked-cluster expansion for the thermodynamic potential with electron–electron interaction as the propagator. The simplest theory with full vertex renormalization, summing self-consistently multiple scatterings from two electron–hole channels, is proposed. We obtain an approximation with a generating functional in closed form enabling us to handle appropriately singularities in two-particle Green functions. The approximation is shown to be asymptotically exact in an external magnetic field close to the fully polarized ferromagnetic state at half-filling and zero temperature.

1. Introduction

Tight-binding models of correlated electrons are expected to provide descriptions of the thermodynamic and spectral properties of the underlying system in the weak-coupling regime as well as in the strong-coupling regime. We have at our disposal relatively reliable techniques for describing the two extreme limits of weak and strong couplings in the archetypal Hubbard model. The weak-coupling regime is governed by a Hartree–Fock mean field with dynamical fluctuations captured by Fermi-liquid theory. Extended systems at low temperatures are Pauli paramagnets with smeared out local magnetic moments. For bipartite lattices, antiferromagnetic long-range order sets in at half-filling and zero temperature at arbitrarily small interaction. In the strong-coupling regime, the Hubbard model at half-filling maps onto a Heisenberg antiferromagnet with pronounced local magnetic moments and the Curie–Weiss law for the staggered magnetic susceptibility, at least at the mean-field level. The spectral structure is dominated by separated lower and upper Hubbard bands and the strongly correlated system seems to be insulating even in the paramagnetic phase.

In recent years, the importance of the region in which the effective Coulomb repulsion is comparable with the kinetic energy, and hence is neither very weak nor very strong, has significantly increased. Unfortunately there has been up to now no adequate method for describing this transition region between the weak- and strong-coupling limits. At intermediate coupling, dynamical fluctuations control the low-temperature physics of interacting electrons, and neither weak-coupling nor atomic-like perturbation theories are

0953-8984/98/132915+18$19.50

adequate. In this non-perturbative regime a singularity in a generic two-particle function is approached and we expect breakdown of the Fermi-liquid regime and a transition to an ordered state or eventually to a Mott insulator in the Hubbard-like models [1].

New progress in the construction of dynamical mean-field theories via high spatial lattice dimensions improved the chances of it being possibile to investigate the transition region between weak and strong coupling [2]. Although the spatial fluctuations are reduced in high dimensions, there is no restriction on the quantum dynamical fluctuations which are important at intermediate coupling. In particular, the quantum Monte Carlo technique in $d = \infty$ dimensions revealed a number of new features of the (disordered) Hubbard model at finite temperatures and intermediate couplings. We have learned of new conclusively demonstrated aspects of the magnetic phase diagram of the finite-temperature Hubbard model [3–6]. However, the quantum Monte Carlo technique is restricted just to relatively high temperatures. That is why an analytic method based on second-order perturbation theory, called IPT, was used to study the transition from weak to strong coupling at zero temperature [7]. IPT at half-filling reproduces well the finite-temperature Monte Carlo data and contains the weak-coupling (up to U^2) and atomic solutions as exact limits. Unlike Hubbard-III-like theories, it reproduces the Fermi liquid at weak coupling. A metal–insulator transition was found at $U_c \approx 6/\pi\nu$, where ν is the DOS at the Fermi level [8–10]. Although IPT is an analytic theory, its solution can be reached only via iterations that depend on the initial value of the self-energy. When we start with $\Sigma^{(0)}(z) = 0$, the iterations converge for weak interaction to a metallic solution. If we start with $\Sigma^{(0)}(z) = \Sigma_{at}(z) = U^2/4z$ we end up with an insulating solution for sufficiently strong interaction. The IPT scheme fails to converge close to the metal–insulator critical point. Different reasoning had to be used to support the existence and character of the zero-temperature metal–insulator transition [11].

Since quantitative description of the Mott–Hubbard metal–insulator transition at intermediate coupling remains analytically inaccessible, attempts have been made to investigate the metal–insulator transition in the Hubbard model exposed to an external magnetic field [12–15]. Perturbation theory breaks down at intermediate and strong coupling close to the instability of the fully polarized ferromagnet. Mean-field analysis *à la* BCS theory of superconductivity [12] can be trusted only in three and more spatial dimensions and deep in the strong-coupling limit with mean-field long-range order. The Hubbard model in $d = 1, 2$ dimensions is in the strong-coupling regime over the whole range of the interaction strength, but shows no mean-field long-range order.

The failure of the existing analytic–numerical methods to describe properly intermediate coupling with the metal–insulator transition at half-filling lies in the inadequate treatment of perturbation theory at two-particle criticality. While the one-particle functions are renormalized, the coupling constant remains mostly unrenormalized. However, the metal–insulator transition and the paramagnet–antiferromagnet transition appear due to condensation of electron–hole pairs and generate a pole in a two-particle Green function. Such a situation demands a theory with full renormalization of the relevant two-particle Green functions.

The aim of this paper is to build up a systematic theory for a reliable description of the two-particle critical behaviour at intermediate and strong coupling of Hubbard-like models. We use a renormalized perturbation expansion based on parquet-type diagrams with non-trivial renormalizations of two-particle functions. In particular, we demonstrate the necessity for dynamical vertex renormalizations whenever we approach a critical point. An approximation with a generating functional, where the one- and two-particle functions are fully renormalized, is proposed for the description of the critical behaviour of condensation of bound electron–hole pairs. It is a simplified version of the parquet algebra keeping only

the potentially most singular contributions to the two-particle scattering functions diverging at the critical point. It strongly renormalizes scatterings within electron–hole pairs and leaves inter-pair correlations unrenormalized. We show that the approximation derived becomes asymptotically exact at zero temperature and half-filling when a fully polarized solution in an external magnetic field is approached. Standard perturbation theory breaks down in this limit and a reliable description can be reached only with full vertex renormalization in the relevant two-particle scattering processes.

The arrangement of the paper is as follows. A systematic self-consistent expansion for intermediate and strong coupling with renormalized two-particle functions is expounded in section 2. To demonstrate the systematics of the general expansion, generating functionals for simple ring and ladder series as well as the FLEX approximation are rederived in section 3. Section 4 points to the necessity for vertex renormalizations in theories near critical points of the two-particle functions in order to comply with a Ward identity binding charge renormalizations (vertices) to mass renormalizations (self-energy). A new approximation with fully renormalized vertex functions having a generating functional in closed form is derived in section 5. Application of the new approximation to the half-filled Hubbard model at zero temperature close to the fully polarized ferromagnetic state is presented in section 6. The last section, section 7, gives the conclusions.

2. A systematic expansion with renormalizations in two-particle Green functions

To study correlated electron systems at intermediate coupling quantitatively, we will resort to the tight-binding Hubbard model. The intermediate coupling in the Hubbard model can be characterized by criticality of a two-particle Green function. Weak-coupling perturbation theory with bare interaction no longer reflects the relevant physics of creation and annihilation of long-living electron–hole pairs. To succeed in the quantitative description of this complex situation, it is necessary to reformulate perturbation theory in such a way that the bare interaction be systematically replaced with fully renormalized two-particle functions determined from multiple two-particle scattering processes. This means that we have to use a perturbation theory at the level of two-particle Green functions.

To develop systematic approximations for one-particle Green functions we use Dyson's equation, enabling us to consider explicitly only one-particle irreducible diagrams contributing to the self-energy. The situation is more complicated at the level of two-particle functions. Although we can use a Bethe–Salpeter equation to extract two-particle irreducible diagrams, we have three possible ways of doing it. We have three channels for multiple two-particle scatterings defining three types of two-particle irreducibility. They are the electron–hole (e–h), electron–electron (e–e) and interaction (U) channels schematically drawn in figure 1. Different channels mean different rearrangements of the perturbation expansion. The chosen irreducible diagrams are summed first and the remaining reducible ones are summed via a Bethe–Salpeter equation at the end. If the perturbation series converges, all rearrangements must lead to the same result.

When studying two-particle functions we need to know the one-particle self-energy. Hence perturbation theory for two-particle functions cannot be developed without a parallel expansion for the self-energy. To approximate the one- and two-particle functions simultaneously, we use perturbation expansion with two-particle functions as a means for developing controllable, comprehensive approximations for a generating thermodynamic potential. All of the physical quantities will then be determined consistently from the generating functional via functional derivatives.

As a first step we decide which is the relevant two-particle function for our purpose to

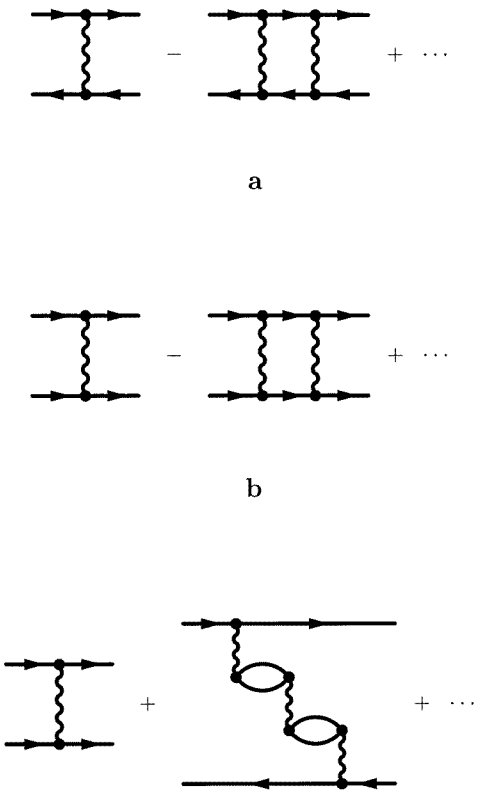

Figure 1. The first few diagrams contributing to the electron–hole, (a), electron–electron, (b), and interaction, (c), channels of the two-particle scattering function.

describe correlated electrons at intermediate and strong coupling. It should be a function approaching a pole with increasing interaction. Such a function must be related to the interaction (two-particle) part of the underlying Hamiltonian. The natural generalization of the Hubbard interaction is the following two-particle function:

$$\mathcal{C}_{ij}(\tau) = \langle \hat{n}_{i\uparrow}(\tau)\hat{n}_{j\downarrow}(0)\rangle - \langle \hat{n}_{i\uparrow}(\tau)\rangle\langle \hat{n}_{j\downarrow}(0)\rangle \tag{1}$$

measuring correlations between spin-up and spin-down densities at different times and different lattice sites. The brackets denote thermal averaging. The Fourier transform $\mathcal{C}(\boldsymbol{q}, \mathrm{i}\nu_m)$ of the above function is a two-particle function approaching a pole when the Hubbard interaction increases. Note that ν_m are bosonic Matsubara frequencies. Due to the space and time translational invariance of the Hamiltonian, $\mathrm{Im}\,\mathcal{C}(\boldsymbol{q}, 0) = 0$ and the real part has a definite sign; that is,

$$\mathcal{C}(\boldsymbol{q}, 0) \propto -U X_{\uparrow\uparrow}(\boldsymbol{q}) X_{\downarrow\downarrow}(\boldsymbol{q}) < 0$$
$$\text{with } X_{\sigma\sigma}(\boldsymbol{q}) = \mathcal{N}^{-1} \sum_{\boldsymbol{k}} \frac{f(\epsilon(\boldsymbol{k}) - \mu_\sigma) - f(\epsilon(\boldsymbol{k}+\boldsymbol{q}) - \mu_\sigma)}{\epsilon(\boldsymbol{k}) - \epsilon(\boldsymbol{k}+\boldsymbol{q})}. \tag{2}$$

This relation is exactly fulfilled at weak coupling and can qualitatively be broken (a change of the sign) only if the function $\mathcal{C}(\boldsymbol{q}, \mathrm{i}\nu_m)$ goes through a pole. The pole would indicate

breakdown of the Fermi liquid. In the weak-coupling, Fermi-liquid regime, we can write

$$\mathcal{C}(\boldsymbol{q},0)=\frac{T}{4}\left[\kappa(\boldsymbol{q},0)-\chi(\boldsymbol{q},0)\right]<0 \tag{3}$$

where $\kappa(\boldsymbol{q},\mathrm{i}\nu_m)$ is the dynamical compressibility and $\chi(\boldsymbol{q},\mathrm{i}\nu_m)$ the dynamical magnetic susceptibility. Equation (3) states that magnetic fluctuations are stronger than the charge fluctuations in the models with the Hubbard repulsive interaction. Divergence in the function $\mathcal{C}(\boldsymbol{q},0)$ induces divergence in the magnetic susceptibility and hence is an indication of a magnetic instability.

The function $\mathcal{C}(\boldsymbol{q},\mathrm{i}\nu_m)$ will be approximated by a selection of classes of Feynman diagrams. According to Baym and Kadanoff [16, 17] a thermodynamically consistent theory must work with fully renormalized one-particle propagators. To construct consistent approximation schemes we have to build up a generating functional $\Phi[U,G]$ from the function $\mathcal{C}(\boldsymbol{q},\mathrm{i}\nu_m)$. To do that we apply a linked-cluster expansion recently proposed by the author and J Schlipf [18]. Its salient feature is that the interaction line (non-relativistic photons) is used for edges (diagram bonds or propagators) and loops of electron Green functions serve as unperturbed vertices. An analogy between the classical free-energy functional of the Ising model $W[J,h]$ and the quantum grand potential $\Omega[U,G^{(0)}]$ is thereby made, i.e. $J\longleftrightarrow U$ and $h\longleftrightarrow G^{(0)}$. We use this analogy to construct the generating functional $\Phi[U,G]$ from the two-particle function $\mathcal{C}(\boldsymbol{q},\mathrm{i}\nu_m)$.

We represent the grand potential of the Hubbard model in the homogeneous phase in the following form:

$$\frac{1}{\mathcal{N}}\Omega[n;\Sigma,G]=-Un_\uparrow n_\downarrow-\frac{1}{\beta\mathcal{N}}\sum_{\sigma n,\boldsymbol{k}}\mathrm{e}^{\mathrm{i}\omega_n 0^+}\{\ln[\mathrm{i}\omega_n+\mu_\sigma-\epsilon(\boldsymbol{k})-Un_{-\sigma}-\Sigma_\sigma(\boldsymbol{k},\mathrm{i}\omega_n)]$$
$$+G_\sigma(\boldsymbol{k},\mathrm{i}\omega_n)\Sigma_\sigma(\boldsymbol{k},\mathrm{i}\omega_n)\}+\Phi[U,G] \tag{4}$$

where n_σ, $\Sigma_\sigma(\boldsymbol{k},\mathrm{i}\omega_n)$, $G_\sigma(\boldsymbol{k},\mathrm{i}\omega_n)$ are variational variables (functions). We introduce a small perturbation $U\to U+\delta U(\boldsymbol{q},\mathrm{i}\nu_m)$. The function $\mathcal{C}(\boldsymbol{q},\mathrm{i}\nu_m)$ is defined as a variational derivative of the generating functional

$$\mathcal{C}(U;\boldsymbol{q},\mathrm{i}\nu_m)=\left.\frac{\delta\Phi[U,G]}{\delta U(\boldsymbol{q},\mathrm{i}\nu_m)}\right|_{\delta U=0}. \tag{5}$$

The linked-cluster theorem is used for the inverse transformation

$$\Phi[U,G]=\frac{U}{\beta\mathcal{N}}\sum_{\boldsymbol{q}m}\int_0^1\mathrm{d}\lambda\;\mathcal{C}(U\lambda|\boldsymbol{q},\mathrm{i}\nu_m). \tag{6}$$

The two-particle function $\mathcal{C}(U\lambda|\boldsymbol{q},\mathrm{i}\nu_m)$ is understood as a functional of the fully renormalized electron propagator $G(\boldsymbol{k},\mathrm{i}\omega_n)$ with the self-energy determined at the interaction strength U.

The function $\mathcal{C}(U|\boldsymbol{q},\mathrm{i}\nu_m)$ does not obey an equation of motion. It is connected with a general two-particle Green function $\mathcal{K}_{\uparrow\downarrow}(U|k',k'';q)$ determined from a set of coupled Bethe–Salpeter equations. To simplify lengthy expressions, we use the four-vector notation $k=(\boldsymbol{k},\mathrm{i}\omega_n)$ and $q=(\boldsymbol{q},\mathrm{i}\nu_m)$ for the fermionic and bosonic variables, respectively. We can write

$$\mathcal{C}(U|\boldsymbol{q},\mathrm{i}\nu_m)=-\frac{1}{\beta^2\mathcal{N}^2}\sum_{k',k''}G_\uparrow(k')G_\uparrow(k'+q)G_\downarrow(k'')G_\downarrow(k''+q)\mathcal{K}_{\uparrow\downarrow}(U|k',k'';q). \tag{7}$$

The functions $\mathcal{K}_{\sigma\sigma'}(k',k'';q)$ can be represented as sums of contributions from different two-particle channels:

$$\mathcal{K}_{\sigma\sigma'}(k,k';q)=I_{\sigma\sigma'}(k,k';q)+\mathcal{K}^U_{\sigma\sigma'}(k,k';q)+\mathcal{K}^{eh}_{\sigma\sigma'}(k,k';q)+\mathcal{K}^{ee}_{\sigma\sigma'}(k,k';q) \tag{8}$$

where $I_{\sigma\sigma'}$ contains diagrams *irreducible* in all of the channels while $\mathcal{K}^{\alpha}_{\sigma\sigma'}$ is a sum of diagrams *reducible* in the particular channel α. Each of the reducible two-particle functions obeys a Bethe–Salpeter equation mixing different channels and eventually spins. The equations in the 'horizontal' electron–hole and electron–electron channels read

$$\mathcal{K}^{eh}_{\sigma\sigma'}(k,k';q) = -\frac{1}{\beta\mathcal{N}}\sum_{q'}\Lambda^{eh}_{\sigma\sigma'}(k,k';q')G_{\sigma}(k+q')G_{\sigma'}(k'+q') \times \mathcal{K}_{\sigma\sigma'}(k+q',k'+q';q-q') \tag{9a}$$

$$\mathcal{K}^{ee}_{\sigma\sigma'}(k,k';q) = -\frac{1}{\beta\mathcal{N}}\sum_{k''}\Lambda^{ee}_{\sigma\sigma'}(k,k+k'+q-k'';k''-k)G_{\sigma}(k'')G_{\sigma'}(k+k'+q-k'') \times \mathcal{K}_{\sigma\sigma'}(k'',k';k+q-k''). \tag{9b}$$

The reducible functions in the 'vertical' or the interaction channel are determined from the equations

$$\mathcal{K}^{U}_{\sigma\sigma'}(k,k';q) = -\frac{1}{\beta\mathcal{N}}\sum_{k''\sigma''}\Lambda^{U}_{\sigma\sigma''}(k,k'';q)G_{\sigma''}(k'')G_{\sigma''}(k''+q)\mathcal{K}_{\sigma''\sigma'}(k'',k';q). \tag{9c}$$

Here $\Lambda^{\alpha}_{\sigma\sigma'}(k,k';q)$ are sums of irreducible diagrams in the αth channel. Equations (9) have the structure of parquet diagrams [19, 20]. To complete the parquet algebra and to close the equations we must add a definition for the irreducible functions from each channel. When no further approximations are used, the parquet equations are completed with a relation between the reducible, $\mathcal{K}^{\alpha}$, and irreducible, Λ^{α}, functions:

$$\Lambda^{\alpha}_{\sigma\sigma'}(k',k'';q') = \mathcal{K}_{\sigma\sigma'}(k',k'';q) - \mathcal{K}^{\alpha}_{\sigma\sigma'}(k',k'';q). \tag{10}$$

The generating functional $\Phi[U,G]$ is now fully determined from the completely irreducible two-particle vertex functions $I_{\sigma\sigma'}(U\lambda|k',k'';q)$, Bethe–Salpeter equations (8)–(10) and linked-cluster theorem (6), with (7). The self-energy is determined from the saddle point of the generating functional Ω with respect to the fermion propagator G. Note that the self-energy here measures only dynamical fluctuations beyond the Hartree approximation.

Although the approximation scheme (6)–(10) is complete we do not have the generating functional in closed form. Any advanced approximation with two- and one-particle renormalizations is of practical use only if we succeed in integrating the linked-cluster theorem explicitly to attain a theory entirely determined by a single interaction strength. Only then can we use the two-particle functions to study the stability and critical behaviour of solutions at intermediate and strong coupling.

3. Simple approximations

As examples of the systematics in the general construction of a perturbation expansion with renormalizations in two-particle Green functions, we sum two-particle scatterings from just a single channel where we can explicitly integrate over the interaction strength in the linked-cluster theorem (6). In all of these approximations the completely irreducible vertex remains unrenormalized, $I_{\uparrow\downarrow} = U$, $I_{\sigma\sigma} = 0$.

3.1. Ring diagrams

We neglect contributions to the two-particle scattering matrix $\mathcal{K}_{\uparrow\downarrow}$ coming from the electron–electron and electron–hole channels and consider explicitly only the interaction channel.

This means that no multiple scatterings are allowed. Moreover, we neglect the irreducible functions for scatterings of quasiparticles with the same spin. We choose

$$\Lambda^{eh}_{\sigma\sigma'} = \Lambda^{ee}_{\sigma\sigma'} = 0 \qquad \Lambda^{\alpha}_{\sigma\sigma} = 0 \tag{11}$$

where $\alpha = U, ee, eh$. The two-particle function $\mathcal{K}_{\uparrow\downarrow}$ in this approximation then reads

$$\mathcal{K}^{Ring}_{\uparrow\downarrow}(U|k', k''; q) = \frac{U}{1 - U^2 X_{\uparrow}(\boldsymbol{q}, \mathrm{i}\nu_m) X_{\downarrow}(\boldsymbol{q}, \mathrm{i}\nu_m)}. \tag{12}$$

The integral over the interaction strength can be performed simply, leading to a generating functional

$$\Phi^{Ring}[U, G] = \frac{1}{2\beta\mathcal{N}} \sum_{\boldsymbol{q}m} \mathrm{e}^{\mathrm{i}\nu_m 0^+} \ln[1 - U^2 X_{\uparrow}(\boldsymbol{q}, \mathrm{i}\nu_m) X_{\downarrow}(\boldsymbol{q}, \mathrm{i}\nu_m)] \tag{13a}$$

where

$$X_{\sigma}(\boldsymbol{q}, \mathrm{i}\nu_m) = \frac{1}{\beta\mathcal{N}} \sum_{\boldsymbol{k}n} G_{\sigma}(\boldsymbol{k}, \mathrm{i}\omega_n) G_{\sigma}(\boldsymbol{k} + \boldsymbol{q}, \mathrm{i}(\omega_n + \nu_m)) \tag{13b}$$

is a bubble of two renormalized one-electron propagators. The self-energy is determined by an integral equation derived from a functional variation of the generating functional $\Phi^{Ring}[U, G]$ w.r.t. the one-electron propagator G. The functional Φ^{Ring} generates a shielded interaction approximation introduced by Baym and Kadanoff [16] and recently investigated in infinite dimensions in [21, 18].

3.2. Ladder diagrams

Other single-channel approximations to the two-particle scattering matrix $\mathcal{K}_{\uparrow\downarrow}$ consist of ladders of either multiple singlet electron–hole or electron–electron scatterings. In these ladder approximations we neglect screening of the interaction due to polarization bubbles of electron–hole pairs. The approximations can be formulated mathematically as

$$\Lambda^{\alpha}_{\sigma\sigma} = \Lambda^{U}_{\uparrow\downarrow} = 0 \qquad \Lambda^{ee}_{\uparrow\downarrow} = 0 \quad \bigvee \quad \Lambda^{eh}_{\uparrow\downarrow} = 0 \tag{14}$$

where the former alternative holds for the electron–hole ladder while the latter holds for the electron–electron one. Summing the geometric series of the only non-trivial Bethe–Salpeter equations, we obtain for the electron–hole channel

$$\mathcal{K}^{RPA}_{\uparrow\downarrow}(U|k, k'; q) = U \Big/ \left(1 + \frac{U}{\beta\mathcal{N}} \sum_{k''} G_{\uparrow}(k - k' + k'') G_{\downarrow}(k'')\right) \tag{15a}$$

and for the electron–electron channel

$$\mathcal{K}^{TMA}_{\uparrow\downarrow}(U|k, k'; q) = U \Big/ \left(1 + \frac{U}{\beta\mathcal{N}} \sum_{k''} G_{\uparrow}(k + k' - k'') G_{\downarrow}(k'')\right). \tag{15b}$$

We can again perform the integration in the linked-cluster theorem (6), and we end up with

$$\Phi^{RPA}[U, G] = -\frac{1}{2\beta\mathcal{N}} \sum_{\boldsymbol{q}m} \mathrm{e}^{\mathrm{i}\nu_m 0^+} \{U X(\boldsymbol{q}, \mathrm{i}\nu_m) - \ln[1 + U X(\boldsymbol{q}, \mathrm{i}\nu_m)]\} \tag{16a}$$

for the electron–hole channel and analogously with

$$\Phi^{TMA}[U, G] = -\frac{1}{2\beta\mathcal{N}} \sum_{\boldsymbol{q}m} \mathrm{e}^{\mathrm{i}\nu_m 0^+} \{U Y(\boldsymbol{q}, \mathrm{i}\nu_m) - \ln[1 + U Y(\boldsymbol{q}, \mathrm{i}\nu_m)]\} \tag{16b}$$

for the electron–electron channel. Here we used the notation

$$X(\boldsymbol{q}, \mathrm{i}\nu_m) = \frac{1}{\beta\mathcal{N}} \sum_{\boldsymbol{k}n} G_\uparrow(\boldsymbol{q}+\boldsymbol{k}, \mathrm{i}\omega_{m+n}) G_\downarrow(\boldsymbol{k}, \mathrm{i}\omega_n) \tag{16c}$$

$$Y(\boldsymbol{q}, \mathrm{i}\nu_m) = \frac{1}{\beta\mathcal{N}} \sum_{\boldsymbol{k}n} G_\uparrow(\boldsymbol{q}-\boldsymbol{k}, \mathrm{i}\omega_{m-n}) G_\downarrow(\boldsymbol{k}, \mathrm{i}\omega_n). \tag{16d}$$

Note that Φ^{RPA} generates random-phase approximation with renormalized propagators, i.e. its renormalized version as introduced by Suhl in the study of the single-impurity Anderson model [22]. The generating functional Φ^{TMA} with multiple electron–electron scatterings describes a renormalized T-matrix approximation studied by Baym and Kadanoff [16].

3.3. The FLEX approximation

One possibility for going beyond the one-channel approximations is to add contributions from separate, topologically inequivalent channels. This is a first (non-self-consistent) step in iterations towards a solution of the general parquet diagrams. The resulting, so-called fluctuation-exchange (FLEX) approximation [23], can be characterized by the choice of the irreducible functions

$$\Lambda^U_{\uparrow\downarrow} = \Lambda^{eh}_{\uparrow\downarrow} = \Lambda^{ee}_{\uparrow\downarrow} = U \qquad \Lambda^\alpha_{\sigma\sigma} = 0. \tag{17}$$

The full two-particle scattering function can be represented as a sum of one-channel functions:

$$\mathcal{K}^{FLEX}_{\uparrow\downarrow} = \mathcal{K}^{Ring}_{\uparrow\downarrow} + \mathcal{K}^{RPA}_{\uparrow\downarrow} + \mathcal{K}^{TMA}_{\uparrow\downarrow} - 2\mathcal{K}^{(2)}_{\uparrow\downarrow} \tag{18}$$

where $\mathcal{K}^{(2)}_{\uparrow\downarrow}$ is the two-particle function in second-order perturbation theory. The generating functional Φ^{FLEX}, being also a sum of functionals of the one-channel approximations

$$\Phi^{FLEX}[U, G] = \Phi^{Ring}[U, G] + \Phi^{RPA}[U, G] + \Phi^{TMA}[U, G] - 2\Phi^{(2)}[U, G] \tag{19}$$

generates the corresponding self-energy of the FLEX approximation.

All of the above-derived approximations are self-consistent at the level of one-particle functions. A series of multiple two-particle scatterings contribute to the self-energy, but the interaction strength in the scattering processes remains unrenormalized. With increasing Coulomb repulsion the two-particle scattering functions of the ring approximation and the RPA show a pole close to half-filling and very low temperatures. The intermediate coupling of the Hubbard model then lies in the critical region of $\mathcal{K}^{Ring}_{\uparrow\downarrow}$ and $\mathcal{K}^{RPA}_{\uparrow\downarrow}$. The irreducible function from the interaction channel becomes singular due to the singularity of the two-particle scattering function from the electron–hole (horizontal) channel and vice versa. Hence the bare interaction in multiple scatterings of each channel must be replaced by a renormalized function from the other channel. Neither the ring approximation nor the RPA (FLEX) can lead to a reliable description of intermediate and strong coupling.

4. The necessity for the full renormalization of the interaction strength at two-particle criticality

The early studies using parquet diagrams in the local-moment problem in metals [19] stressed the necessity of going beyond the renormalized RPA of Suhl and including vertex renormalizations in the two-particle scatterings. The simple ring and ladder approximations renormalize only the self-energy and use the unrenormalized interaction strength U in the

two-particle scattering processes. It is clear that at intermediate and strong coupling, the actual interaction that the quasiparticles 'feel' in their mutual scattering events must be renormalized by the presence of other quasiparticle pairs. In fact, we have to replace the bare interaction U by a renormalized two-particle function $\mathcal{K}_{\uparrow\downarrow}$ from (2) projected to the respective channel. We will do this systematically in the next section.

However, there is a more basic reason for introducing a vertex renormalization whenever we use a mass renormalization. There is a relation between a two-particle function and a derivative of the one-particle propagator having the structure of a Ward identity. Baym and Kadanoff formulated necessary conditions for a many-body theory to fulfil mass conservation. A generalized Ward identity connecting an irreducible vertex function with a variation of the self-energy with respect to an external potential was thereby derived [17]. An interacting electron system contains not only mass but also charge. The electron–electron interaction carries an electrostatic energy $U = e^2/a^*$. In closed systems the electrostatic potential is generated entirely by the actual charge distribution. The charge is carried exclusively by the particles involved. Hence a redistribution of mass density must be accompanied by a corresponding charge redistribution in order not to generate spurious sources of the electrostatic potential. This 'charge conservation', i.e. the entire electrostatic potential, is generated from the charge distribution only, and can be expressed for the Hubbard interaction as a 'Ward identity':

$$\frac{\partial\Omega(U,\mu_{i\sigma})}{\partial U} = \sum_i \left[\frac{\delta^2\Omega}{\delta\mu_{i\uparrow}\,\delta\mu_{i\downarrow}} + \frac{\delta\Omega}{\delta\mu_{i\uparrow}}\frac{\delta\Omega}{\delta\mu_{i\downarrow}}\right] = \sum_i \left\{\frac{T}{4}[\kappa_{ii} - \chi_{ii}] + n_{i\uparrow}n_{i\downarrow}\right\} \tag{20a}$$

with the grand potential Ω defined in (4) and κ_{ii}, χ_{ii} as the static, local compressibility and susceptibility, respectively. We can generalize this static identity using small space and time inhomogeneous perturbations $U \to U + \delta U_{ij}(\tau,\tau')$ and $\mu_\sigma \to \mu_\sigma + \delta\mu_{i\sigma}(\tau)$ to obtain

$$\left.\frac{\delta\Phi[U,G]}{\delta U_{ij}(\tau,\tau')}\right|_{\delta U=0,\delta\mu=0} = -\left.\frac{\delta G_{ii\uparrow}(\tau,\tau^+)}{\delta\mu_{j\downarrow}(\tau')}\right|_{\delta U=0,\delta\mu=0}. \tag{20b}$$

Both of these identities are fulfilled for an exact solution. The left-hand side of (20*b*) is the fundamental two-particle function for which the explicit linked-cluster expansion is used. The right-hand side of (20*b*) makes a connection to the dynamical susceptibility and compressibility obtained as variations of the one-particle Green function. The left-hand side of (20*b*) is a variation of the charge distribution and the right-hand side the corresponding variation of mass. If (20*b*) is violated we cannot refer to inequality (3). Identity (20*b*) is important for the linked-cluster expansion where it is used as a fundamental tool for the construction of the generating functional, i.e. for explicit integration in the linked-cluster theorem (6) [24]. However, even for classical spin systems, where the situation is much easier, it was impossible to integrate (20*b*) in full and to resolve the generating functional Φ completely [25].

Most of the existing self-consistent approximations renormalize only mass, i.e. use renormalized one-electron propagators neglecting vertex renormalization. The Ward identity (4) is always violated in self-consistent theories that do not renormalize the interaction strength. For example, for the Hartree approximation we obtain after a Fourier transformation

$$\left.\frac{\delta G_\uparrow^{Hartree}}{\delta\mu_\downarrow}(\boldsymbol{q},\mathrm{i}\nu_m)\right|_{\delta U=0,\delta\mu=0} = UX_\uparrow(\boldsymbol{q},\mathrm{i}\nu_m)X_\downarrow(\boldsymbol{q},\mathrm{i}\nu_m)\left[1 - U^2X_\uparrow(\boldsymbol{q},\mathrm{i}\nu_m)X_\downarrow(\boldsymbol{q},\mathrm{i}\nu_m)\right]^{-1} \tag{21}$$

with the Hartree one-electron propagators. Since $\Phi^{Hartree} \equiv 0$, identity (20*b*) is violated by terms proportional to U, the small expansion parameter of the Hartree approximation. Violation of 'charge conservation' in the Hartree approximation has no qualitative impact on the physics of the solution unless there is a phase transition making the right-hand side of (21) diverge. We hence cannot rely upon the Hartree approximation at critical points. The Hartree phase diagram must be confirmed by a more advanced approximation complying better with charge conservation—at least in such a manner that both sides of (20*b*) lead to qualitatively the same phase diagram.

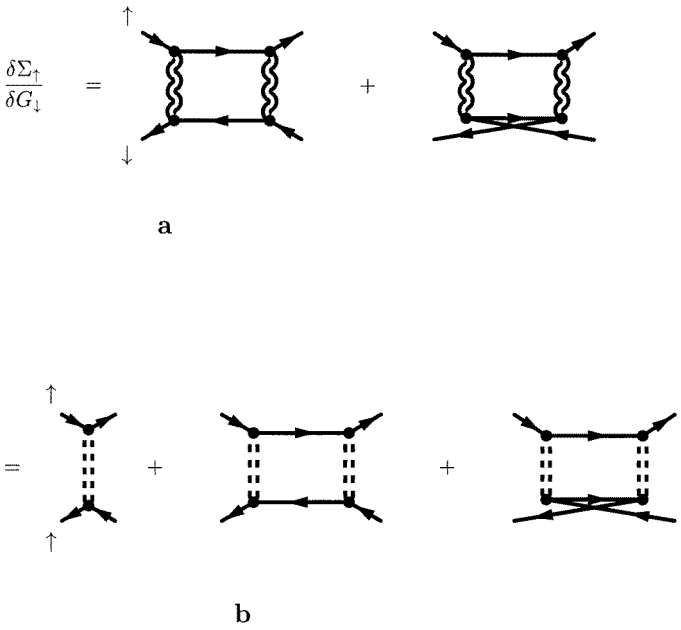

Figure 2. The new vertex functions generated from functional derivatives of the self-energy from the ring diagrams. The double wavy line is the interaction between spin-up and spin-down particles, and the double dashed line the interaction between the particles with the same spin renormalized by ring diagrams. These vertex functions are not contained in the left-hand side of identity (20*b*) of the ring diagrams.

To improve upon the Hartree approximation towards charge conservation we can use the right-hand side of (21) for determination of the generating functional $\Phi[U, G]$ from the linked-cluster theorem. We end up with a generating functional of the ring diagrams investigated in section 3.1. Since this approximation does not contain dynamical vertex renormalizations either, we cannot expect the Ward identity (20) to be fulfilled [26]. The left-hand side of (20*b*) for the ring diagrams is identical to the right-hand side of (21) where the Hartree propagators are replaced by those from the ring diagrams. The new right-hand side of (20*b*) for the ring diagrams must be determined from a set of integral equations and becomes a functional of irreducible vertex functions $\delta\Sigma_\sigma/\delta G_{\sigma'}$. It contains first ladder terms with interaction lines renormalized due to the electron–hole polarization bubbles plotted in figure 2. We see that to comply with charge conservation, at least all ladder and ring diagrams must be taken into account. We can conclude from these few steps that only the parquet diagrams can be expected to obey the Ward identity due to charge conservation.

However, the full parquet algebra is very complicated and does not allow for a general self-consistent (non-perturbative) solution. If all simpler approximations break the identity (20), we may ask how much the violation of charge conservation matters. It is physically *unacceptable* if the functions from the right- and left-hand sides of equation (20) generate *qualitatively* different phase diagrams and lead to incompatible spectral properties. We can trust an approximation violating (20) only if both sides of (20) are qualitatively equivalent.

5. Beyond simple ring and ladder series: dipole approximation

It follows from the preceding analysis that the full parquet approximation would be an ideal candidate for a theory adequately describing two-particle criticality at intermediate coupling. It renormalizes the interaction strength to comply with charge conservation, at least qualitatively. We learned, however, that only non-perturbative solutions, treating singularities of two-particle functions at intermediate coupling analytically, can lead to numerically stable solutions. Parquet diagrams were suggested in the local-moment problem as improvements of Suhl's random-phase approximation. Since no exact solutions to the parquet equations exist, approximations had to be used. The local (static) *ansatz* chosen in [19] failed to reproduce the Kondo scale at strong coupling and to capture the actual strong-coupling behaviour of the parquet diagrams. Neither did non-self-consistent analysis of the divergent diagrams at strong coupling [27] help in the selection of the relevant classes of diagrams.

To achieve a feasible approximation adequate for the description of intermediate coupling and the metal–insulator transition, we have to start with a reduced parquet algebra that, unlike the simple series, treats the two-particle functions from the horizontal and vertical channels equivalently, at least as regards singularities. Since the electron–hole and interaction channels contribute the same divergence (up to a numerical factor) at the critical point of the spin-symmetric case, we must keep contributions to the parquet diagrams from these two channels unabridged. Also, in a spin-polarized situation (in an external magnetic field) close to half-filling, the electron–hole ladders and rings remain dominant.

In the critical region of the metal–insulator transition we expect electrons and holes to form pairs of almost bound states. This means that if an electron and a hole get close to each other they tend to stay together for macroscopically long times. The probability of mutual scatterings of electrons and holes is hence much higher than that of other scattering events. The *intra-pair* scatterings of the electron and hole from the binding pairs are pronounced and are mediated by a renormalized interaction due to the presence of other almost bound electron–hole pairs. The pairs have the total charge zero and carry only a dipole electrical moment. The *inter-pair* interaction is of dipole character and hence weak. There is no significant renormalization of the electrostatic potential due to the scarcity of interaction processes between pairs or pairs and unbound particles. The dipole approximation hence systematically neglects all multiple scatterings where more than two particles take part.

This intuitive physical picture can be formulated mathematically in terms of specific approximations in the general parquet algebra (9). We neglect the three-particle and higher-order irreducible diagrams as irrelevant at the metal–insulator transition. Next, we ignore the triplet irreducible functions. This restriction does not mean that the triplet pairing is absent. It is actually present, but the triplet electron–hole pairs participate *only* in the screening of the interaction strength in the multiple scatterings of the singlet electron–hole pairs. With these restrictions we can set in the asymptotic limit of the transition:

$$I_{\sigma\sigma}(k,k';q)=U \qquad I_{\sigma\sigma}(k,k';q)=0 \qquad \Lambda^{\alpha}_{\sigma\sigma}(k,k';q)=0 \tag{22a}$$

where $\alpha = U, ee, eh$. Strictly speaking, this *ansatz* is not fully mathematically consistent. Because of the mixing of spins, the singularity from the singlet channel also infiltrates the irreducible functions $\Lambda^{\alpha}_{\sigma\sigma}$. These induced singularities are less important than the primary source of divergencies, the singlet irreducible functions $\Lambda^{\alpha}_{\uparrow\downarrow}$.

We now define the singlet two-particle function from the vertical channel as

$$\Gamma_{\uparrow\downarrow}(k, k'; q) = U + \mathcal{K}^{U}_{\uparrow\downarrow}(k, k'; q).$$

It is a functional of the two-particle scattering function from the horizontal channel defined as

$$\Lambda^{U}_{\uparrow\downarrow}(k, k'; q) = \mathcal{K}^{h}_{\uparrow\downarrow}(k, k'; q) = U + \mathcal{K}^{eh}_{\uparrow\downarrow}(k, k'; q) + \mathcal{K}^{ee}_{\uparrow\downarrow}(k, k'; q). \tag{22b}$$

After a few manipulations we obtain

$$\Gamma_{\uparrow\downarrow}(k, k'; q) = U + \frac{1}{\beta^2\mathcal{N}^2}\sum_{k_\uparrow, k_\downarrow} \mathcal{K}^{h}_{\uparrow\downarrow}(k, k_\downarrow; q) G_\downarrow(k_\downarrow) G_\downarrow(k_\downarrow + q) \mathcal{K}^{h}_{\downarrow\uparrow}(k_\uparrow + q, k_\downarrow + q; -q)$$
$$\times\, G_\uparrow(k_\uparrow) G_\uparrow(k_\uparrow + q) \left[\mathcal{K}^{h}_{\uparrow\downarrow}(k_\uparrow, k'; q) - U + \Gamma_{\uparrow\downarrow}(k_\uparrow, k'; q)\right]. \tag{22c}$$

The function $\Gamma_{\uparrow\downarrow}(k, k'; q)$ shows divergence for $\boldsymbol{q} = \boldsymbol{q}_0$ and $\nu \to 0$ in the critical region of condensation of electron–hole (triplet) pairs as in the ring approximation. However, the character of the pole is significantly influenced by the non-trivial dependence of the function $\Gamma_{\uparrow\downarrow}$ on the momenta of the participating fermions. The renormalized interaction $\Gamma_{\uparrow\downarrow}$ from (22*c*) represents a sum of diagrams each with a single outer interaction line from each side. That is, multiple connections between pairs that are almost bound are disregarded. Typical diagrams included and omitted in the renormalized interaction are plotted in figure 3.

To complete the approximation, we must specify the two-particle function from the horizontal channel. It is determined from equations (9*a*) and (9*b*) with appropriate irreducible functions. Since multiple electron–electron scatterings are not supposed to contribute divergent terms in the critical region of the metal–insulator transition, we can neglect these scatterings completely without affecting the leading-order asymptotics. We put

$$\Lambda^{ee}_{\uparrow\downarrow}(k, k'; q) = 0. \tag{23a}$$

With this simplification we gain an explicit integral equation for the two-particle scattering function from the horizontal channel. We have

$$\mathcal{K}^{h}_{\uparrow\downarrow}(k, k'; q) = U - \frac{1}{\beta\mathcal{N}}\sum_{q'} \Gamma_{\uparrow\downarrow}(k, k'; q') G_\uparrow(k + q') G_\downarrow(k' + q')$$
$$\times\, \left[\Gamma_{\uparrow\downarrow}(k + q', k' + q'; q - q') - U + \mathcal{K}^{h}_{\uparrow\downarrow}(k + q', k' + q'; q - q')\right]. \tag{23b}$$

The function $\mathcal{K}^{h}_{\uparrow\downarrow}$ shows a pole at the transition with condensation of electron–hole (singlet) pairs—but here for $\boldsymbol{k}' - \boldsymbol{k} = \boldsymbol{q}_0$ and $\omega' - \omega \to 0$, as in the simple ladder approximation (RPA). However, the critical behaviour at the pole becomes more complex due to a richer structure of $\mathcal{K}^{h}_{\uparrow\downarrow}(k, k'; q)$.

The two-particle part of the dipole approximation is now complete, i.e. (22) and (23) fully characterize the necessary two-particle functions. However, as already mentioned in section 2, an approximation for two-particle functions is practicable only if it allows for explicit integration over the interaction strength in the linked-cluster theorem needed for the construction of the generating functional $\Phi[U, G]$. Using the renormalized two-particle functions $\Gamma_{\uparrow\downarrow}$ and $\mathcal{K}^{h}_{\uparrow\downarrow}$ we can construct a generating functional of the dipole approximation in closed form. First we use relation (7) where we rewrite the full two-particle scattering

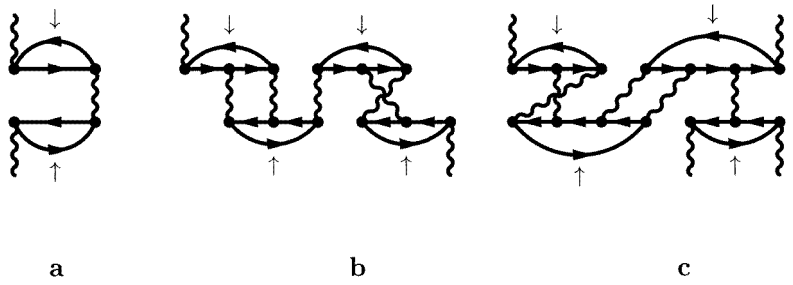

a **b** **c**

Figure 3. Typical diagrams contributing to $\Gamma_{\uparrow\downarrow}$, (a), (b), where no more than two particles take part in multiple scatterings from the irreducible function Λ^U. Diagram (c) does not contribute to $\Gamma_{\uparrow\downarrow}$, since more than two external interaction lines are attached.

function with the aid of solutions from the horizontal and vertical channels. The function $\mathcal{C}$ in our simplified parquet algebra explicitly reads

$$\mathcal{C}(q) = -\frac{1}{\beta^2\mathcal{N}^2}\sum_{k',k''} G_\uparrow(k')G_\uparrow(k'+q)G_\downarrow(k'')G_\downarrow(k''+q) \times \left[\mathcal{K}^h_{\uparrow\downarrow}(k',k'';q) + \Gamma_{\uparrow\downarrow}(k',k'';q) - U\right]. \tag{24}$$

Next we introduce the following notation and operations:

$$[X_{\uparrow\downarrow}G_\uparrow G_\downarrow](k,k';q) \equiv X_{\uparrow\downarrow}(k,k';q)G_\uparrow(k+q)G_\downarrow(k'+q) \tag{25a}$$

$$[X \star Y](k,k';q) \equiv \frac{1}{\beta\mathcal{N}}\sum_{q'} X(k,k';q')Y(k+q',k'+q';q-q') \tag{25b}$$

$$[X_{\uparrow\downarrow}G_\downarrow G_\downarrow \bullet X_{\downarrow\uparrow}G_\uparrow G_\uparrow](k,k';q) \equiv \frac{1}{\beta\mathcal{N}}\sum_{k''} X_{\uparrow\downarrow}(k,k'';q)G_\downarrow(k'')G_\downarrow(k''+q) \times X_{\downarrow\uparrow}(k'+q,k''+q;-q)G_\uparrow(k')G_\uparrow(k'+q) \tag{25c}$$

$$[X \circ Y](k,k';q) \equiv \frac{1}{\beta\mathcal{N}}\sum_{k''} X(k,k'';q)Y(k'',k';q). \tag{25d}$$

Using these definitions we integrate the linked-cluster theorem to a generating functional $\Phi[U;\Gamma_{\uparrow\downarrow},\mathcal{K}^h_{\uparrow\downarrow};G]$ in the following form:

$$\begin{aligned}\Phi[U;\Gamma_{\uparrow\downarrow},\mathcal{K}^h_{\uparrow\downarrow};G] = {} & \frac{1}{2\beta^3\mathcal{N}^2}\sum_{k,k',q}[(\Gamma_{\uparrow\downarrow}+\mathcal{K}^h_{\uparrow\downarrow}-U)G_\uparrow G_\downarrow](k,k';q) \\ & \times [(\Gamma_{\uparrow\downarrow}+\mathcal{K}^h_{\uparrow\downarrow}-U)G_\uparrow G_\downarrow](k+q,k'+q;-q) \\ & - \frac{1}{2\beta^2\mathcal{N}}\sum_{k,k'}\left\{[\Gamma_{\uparrow\downarrow}G_\uparrow G_\downarrow](k,k';0) - \ln[1+[\Gamma_{\uparrow\downarrow}G_\uparrow G_\downarrow]\star](k,k';0)\right\} \\ & + \frac{1}{2\beta^2\mathcal{N}}\sum_{k,q}\ln\left[1-[\mathcal{K}^h_{\uparrow\downarrow}G_\downarrow G_\downarrow \bullet \mathcal{K}^h_{\downarrow\uparrow}G_\uparrow G_\uparrow]\circ\right](k,k+q;-q).\end{aligned} \tag{26}$$

The first expression on the right-hand side of (26) is a correction due to multiple summation of second-order contributions from the last two terms standing for the ladder, electron–hole scatterings (the second term) and for the rings of electron–hole bubbles (the third term). Unlike the simple series, the bare interaction in the scattering processes is replaced by a fully renormalized two-particle function from the complementary channel. The

generating functional $\Phi[U;\Gamma_{\uparrow\downarrow},\mathcal{K}^h_{\uparrow\downarrow};G]$ contains only fully renormalized one- and two-particle functions. The bare interaction stands for higher-order irreducible functions that remain unrenormalized (neglected) in this approximation.

It is easy to verify that generating functional (26) leads to the reduced parquet equations of the dipole approximation (22*c*) and (23*b*) if we make variations of $\Phi[U;\Gamma_{\uparrow\downarrow},\mathcal{K}^h_{\uparrow\downarrow};G]$ w.r.t. $\mathcal{K}^h_{\uparrow\downarrow}$ and $\Gamma_{\uparrow\downarrow}$, respectively. We can also check by inspection that (5) is fulfilled by functional (26) together with (24).

Variation of the generating functional w.r.t. the one-electron propagator leads to a generic equation for the self-energy if the equations for $\Gamma_{\uparrow\downarrow}$ and $\mathcal{K}^h_{\uparrow\downarrow}$ are used:

$$\Sigma_\uparrow(k) = -\frac{U}{\beta^2\mathcal{N}^2}\sum_{k',q} G_\uparrow(k+q)G_\downarrow(k')G_\downarrow(k'+q)\left[\Gamma_{\uparrow\downarrow}(k,k';q)+\mathcal{K}^h_{\uparrow\downarrow}(k,k';q)-U\right]. \tag{27}$$

Equations (22)–(27) fully determine thermodynamic as well as spectral properties of the dipole approximation for arbitrary interaction. They represent an asymptotic solution of the parquet diagrams in the critical region of a transition point, $U \nearrow U_c$, where electron–hole singlet and triplet bound pairs condense.

6. Application: the Hubbard model in an external magnetic field

In the spin-symmetric case there is no difference between singlet and triplet pairs and the two-particle functions $\Gamma_{\uparrow\downarrow}$ and $\mathcal{K}^h_{\uparrow\downarrow}$ develop the same singularity at the metal–insulator transition. This fact makes it very difficult to apply the dipole approximation directly to the intermediate coupling in the paramagnetic phase. We can, however, apply the dipole approximation more easily to the Hubbard model in an external magnetic field. The parquet approximation becomes asymptotically exact when the fully polarized ferromagnetic state in an external magnetic field is approached. If we resort to half-filling, the leading deviation from the saturated ferromagnet is determined by the dipole approximation. For the sake of simplicity we will explicitly analyse only the one-dimensional case.

An external magnetic field breaks the equivalence between loops of electrons and holes with parallel and antiparallel spins. The degeneracy in the critical region of the metal–insulator transition is thereby lifted. The functions $\Gamma_{\uparrow\downarrow}$ and $\mathcal{K}^h_{\uparrow\downarrow}$ are no longer equivalent and can be treated separately. However, both of them are relevant at intermediate and strong coupling where perturbation theory becomes singular.

We denote the external magnetic field as B. The one-electron propagators can be represented as

$$G_\uparrow(\boldsymbol{k},z) = \left[z+B+\frac{U}{2}-\epsilon(\boldsymbol{k})\right]^{-1} \qquad G_\downarrow(\boldsymbol{k},z) = \left[z-B-\frac{U}{2}-\epsilon(\boldsymbol{k})\right]^{-1}. \tag{28}$$

The electron–hole bubbles in the spin-polarized case have the following representation:

$$X^B_{\uparrow\downarrow}(\boldsymbol{q},\zeta) = X^B_{\downarrow\uparrow}(-\boldsymbol{q},-\zeta) = \frac{1}{\mathcal{N}}\sum_{\boldsymbol{k}}\frac{f(\epsilon(\boldsymbol{k})-B-U/2)-f(\epsilon(\boldsymbol{k}+\boldsymbol{q})+B+U/2)}{\zeta-2B-U+\epsilon(\boldsymbol{k})-\epsilon(\boldsymbol{k}+\boldsymbol{q})} \tag{29a}$$

$$X^B_{\uparrow\uparrow}(\boldsymbol{q},\zeta) = \frac{1}{\mathcal{N}}\sum_{\boldsymbol{k}}\frac{f(\epsilon(\boldsymbol{k})-B-U/2)-f(\epsilon(\boldsymbol{k}+\boldsymbol{q})-B-U/2)}{\zeta+\epsilon(\boldsymbol{k})-\epsilon(\boldsymbol{k}+\boldsymbol{q})} \tag{29b}$$

$$X^B_{\downarrow\downarrow}(\boldsymbol{q},\zeta) = \frac{1}{\mathcal{N}}\sum_{\boldsymbol{k}}\frac{f(\epsilon(\boldsymbol{k})+B+U/2)-f(\epsilon(\boldsymbol{k}+\boldsymbol{q})+B+U/2)}{\zeta+\epsilon(\boldsymbol{k})-\epsilon(\boldsymbol{k}+\boldsymbol{q})}. \tag{29c}$$

At zero temperature and for a sufficiently strong magnetic field, the triplet bubbles $X^B_{\sigma\sigma}$ vanish and the solution to the dipole (parquet) approximation reduces to

$$\Gamma_0 = U \qquad \mathcal{K}_0^h(\boldsymbol{q}, \zeta) = \frac{U}{1 + U X^B_{\uparrow\downarrow}(\boldsymbol{q}, \zeta)}. \tag{30}$$

The critical field for which all the spins will be aligned along the external magnetic field is defined at weak coupling ($U < U_c$) as

$$B_c + \frac{U}{2} = w \tag{31a}$$

where w is the half-bandwidth. At strong coupling the critical field must be determined from [12–15]

$$1 + U X^{B_c}_{\uparrow\downarrow}(\boldsymbol{Q}, 0) = 0 \tag{31b}$$

where $\boldsymbol{Q} = (\pi, \pi, \ldots, \pi)$ is the vector from the Brillouin zone at which the singlet bubble $X_{\uparrow\downarrow}$ reaches its maximum. It is easy to verify that (30) is a solution to the dipole approximation for $B \geqslant B_c$. This is a consequence of the fact that $X_{\uparrow\downarrow}$ has a cut only along the positive real axis, which causes vanishing of the corrections to the bare interaction in the vertical channel.

We now turn to the spatial dimension $d = 1$. The critical interaction separating the weak- and strong-coupling regimes $U_c = 0$. The condition (31b) for the instability of the saturated ferromagnet is simultaneously a condition on a singularity in the two-particle function $\mathcal{K}^h_{\uparrow\downarrow}$. This means that perturbation expansion in $\Delta B = B_c - B$ below the critical magnetic field involves a singular function. Weak-coupling perturbation theory and the Landau mean-field theory of phase transitions break down and one has to introduce renormalizations into the two-particle functions.

If we decrease the magnetic field below its critical value, the function $\mathcal{K}_0^h(Q, \zeta)$ gets a narrow cut on the negative real axis. Without renormalization in the function $\Gamma_{\uparrow\downarrow}$, the staggered susceptibility becomes negative and the spins must antiferromagnetically order. However, below the critical magnetic field the two-particle function $\Gamma_{\uparrow\downarrow}$ is no longer unrenormalized. The leading contribution to this function in ΔB and in the first iteration of the full self-consistency reads

$$\begin{aligned}\delta\Gamma_{\uparrow\downarrow}(k, \mathrm{i}\omega, k', \mathrm{i}\omega'; q, \mathrm{i}\nu) = \int_{-\pi}^{\pi} \frac{\mathrm{d}q'}{2\pi}\, \frac{\mathrm{d}q''}{2\pi} \int_{-\infty}^{\infty} \frac{\mathrm{d}\nu'}{2\pi}\, \frac{\mathrm{d}\nu''}{2\pi}\, \mathcal{K}_0^h(q', \mathrm{i}\nu') \\ \times\, G_\downarrow(k + q', \mathrm{i}\omega + \mathrm{i}\nu') G_\downarrow(k' + q', \mathrm{i}\omega' + \mathrm{i}\nu') \mathcal{K}_0^h(q' - q'', \mathrm{i}\nu' - \mathrm{i}\nu'') \\ \times\, G_\uparrow(k + q'', \mathrm{i}\omega + \mathrm{i}\nu'') G_\uparrow(k' + q'', \mathrm{i}\omega' + \mathrm{i}\nu'') \mathcal{K}_0^h(q - q'', \mathrm{i}\nu - \mathrm{i}\nu'').\end{aligned} \tag{32}$$

For the evaluation of the above expression we need a low-energy expansion for the singular function $\mathcal{K}_0^h$. We obtain for small frequencies and momenta

$$\mathcal{K}_0^h(q, \zeta) = -\frac{1}{X'} \frac{1}{2\,\Delta B + \zeta - X''/X' q^2} \tag{33}$$

where the expansion parameters introduced read

$$\begin{aligned} X' &= \int_{-w}^{w} \mathrm{d}\epsilon\, \frac{\rho(\epsilon)}{(2B + U - 2\epsilon)^2} \\ X'' &= \int_{-w}^{w} \mathrm{d}\epsilon\, \frac{\rho(\epsilon)}{(2B + U - 2\epsilon)^2} \left[\epsilon - \frac{w^2 - \epsilon^2}{2B + U - 2\epsilon}\right]. \end{aligned} \tag{34}$$

In leading order of ΔB the cut on the negative real axis contributes only once and its contribution can be evaluated using representation (33). The correction to the two-particle function from the vertical channel is then

$$\begin{aligned}\delta\Gamma_{\uparrow\downarrow}(k,\mathrm{i}\omega,k',\mathrm{i}\omega';q,\mathrm{i}\nu) = &-\frac{1}{\pi}\sqrt{\frac{\Delta B}{X'X''}}G_\downarrow(k,\mathrm{i}\omega)G_\downarrow(k',\mathrm{i}\omega')\\ &\times\int_{-\pi}^{\pi}\frac{\mathrm{d}q'}{2\pi}\int_{-\infty}^{\infty}\frac{\mathrm{d}\nu'}{2\pi}\,\mathcal{K}_0^h(-q',-\mathrm{i}\nu')\\ &\times G_\uparrow(k+q',\mathrm{i}\omega+\mathrm{i}\nu')G_\uparrow(k'+q',\mathrm{i}\omega'+\mathrm{i}\nu')\mathcal{K}_0^h(q-q',\mathrm{i}\nu-\mathrm{i}\nu'). \qquad (35)\end{aligned}$$

Having the asymptotic behaviour of the function $\Gamma_{\uparrow\downarrow}$, we can evaluate the asymptotics of the function $\mathcal{K}^h_{\uparrow\downarrow}$. It, however, cannot be treated perturbatively, since the unperturbed function $\mathcal{K}^h_0$ is singular. The asymptotic solution in the limit $\Delta B\to 0$ can be represented with the aid of a linear integral equation:

$$\begin{aligned}\mathcal{K}^h_{\uparrow\downarrow}(k,\mathrm{i}\omega,k',\mathrm{i}\omega';q,\mathrm{i}\nu) = &\,U\Big[1-\delta\varphi(k,\mathrm{i}\omega,k',\mathrm{i}\omega';q,\mathrm{i}\nu)\Big]\\ &-\int_{-\pi}^{\pi}\frac{\mathrm{d}q'}{2\pi}\int_{-\infty}^{\infty}\frac{\mathrm{d}\nu'}{2\pi}\,\Big[U+\delta\Gamma_{\uparrow\downarrow}(k,\mathrm{i}\omega,k',\mathrm{i}\omega';q',\mathrm{i}\nu')\Big]\\ &\times G_\uparrow(k+q',\mathrm{i}\omega+\mathrm{i}\nu')G_\downarrow(k'+q',\mathrm{i}\omega'+\mathrm{i}\nu')\\ &\times\mathcal{K}^h_{\uparrow\downarrow}(k+q',\mathrm{i}\omega+\mathrm{i}\nu',k'+q',\mathrm{i}\omega'+\nu';q-q',\mathrm{i}\nu-\mathrm{i}\nu') \qquad (36)\end{aligned}$$

that becomes singular at the critical magnetic field $B=B_c$. We used the notation

$$\begin{aligned}\delta\varphi(k,\mathrm{i}\omega,k',\mathrm{i}\omega';q,\mathrm{i}\nu) = &\int_{-\pi}^{\pi}\frac{\mathrm{d}q'}{2\pi}\int_{-\infty}^{\infty}\frac{\mathrm{d}\nu'}{2\pi}\,G_\uparrow(k+q',\mathrm{i}\omega+\mathrm{i}\nu')G_\downarrow(k'+q',\mathrm{i}\omega'+\mathrm{i}\nu')\\ &\times\delta\Gamma_{\uparrow\downarrow}(k+q',\mathrm{i}\omega+\mathrm{i}\nu',k'+q',\mathrm{i}\omega'+\mathrm{i}\nu';q-q',\mathrm{i}\nu-\mathrm{i}\nu').\end{aligned}$$

Equation (36) can be solved in leading order of ΔB with

$$\mathcal{K}^h_{\uparrow\downarrow}(k,\mathrm{i}\omega,k',\mathrm{i}\omega';q,\mathrm{i}\nu) = \frac{U\left[1-\delta\varphi(k,\mathrm{i}\omega,k',\mathrm{i}\omega';q,\mathrm{i}\nu)\right]}{1+UX_{\uparrow\downarrow}(k-k',\mathrm{i}\omega-\mathrm{i}\omega')+\delta\psi(k,\mathrm{i}\omega,k',\mathrm{i}\omega')} \qquad (37)$$

where

$$\begin{aligned}\delta\psi(k,\mathrm{i}\omega,k',\mathrm{i}\omega') = &\int_{-\pi}^{\pi}\frac{\mathrm{d}q'}{2\pi}\int_{-\infty}^{\infty}\frac{\mathrm{d}\nu'}{2\pi}\,\delta\Gamma_{\uparrow\downarrow}(k,\mathrm{i}\omega,k',\mathrm{i}\omega';q',\mathrm{i}\nu')\\ &\times G_\uparrow(k+q',\mathrm{i}\omega+\mathrm{i}\nu')G_\downarrow(k'+q',\mathrm{i}\omega'+\mathrm{i}\nu').\end{aligned}$$

The two-particle functions $\mathcal{K}^h_{\uparrow\downarrow}$ and $\delta\Gamma_{\uparrow\downarrow}$ can be used in (27) to determine the self-energy and the deviation of the magnetization $\Delta m = 1-m$. They are both proportional to $\sqrt{\Delta B}$ in accord with the Bethe *ansatz* solution [28].

There are two contributions in the denominator of the solution in (37). One, proportional to U, depends on ΔB *linearly* and is negative. The other one, proportional to $\delta\Gamma_{\uparrow\downarrow}$, increases below the critical magnetic field as $\sqrt{\Delta B}$ and is *positive*. Hence the total change is dominated by the renormalization of the interaction strength in the vertical channel $\delta\Gamma_{\uparrow\downarrow}$ stabilizing the disordered state. Only if the total change of $\mathcal{K}^h_{\uparrow\downarrow}$ were positive would the long-range antiferromagnetic order set in. The mean-field term with U has at strong coupling the same structure in all dimensions, while the correction $\delta\Gamma_{\uparrow\downarrow}$ grows at strong coupling and higher dimensions as $\Delta B^{d/2}$. We can hence conclude that the mean-field analysis of reference [12] qualitatively holds in three and higher spatial dimensions in the strong-coupling regime, $U>U_c$. The renormalization $\delta\Gamma_{\uparrow\downarrow}$ plays an important role in high spatial dimensions for $U\leqslant U_c$, i.e. at the metal–insulator transition and at weak coupling with

$B + U/2 < w$, where the asymptotics significantly differs from the strong-coupling one. The metal–insulator transition and the weak-coupling asymptotics in $d = 3$ dimensions will be investigated in a separate publication.

The Hubbard model in two dimensions deserves special attention. The vertex correction $\delta\Gamma_{\uparrow\downarrow}$ in $d = 2$ dimensions is of the same order as the mean-field U-term in integral equation (36). Whether a long-range antiferromagnetic order can set in when there is an external magnetic field may depend on the lattice structure and on the interaction strength. However, to reach an accurate answer we have to include also next-to-leading-order terms neglected in the dipole approximation but included in the complete parquet algebra.

7. Conclusions

We analysed in this paper correlated electron systems at intermediate coupling. We showed that in models with on-site Coulomb repulsion a pole in a characteristic two-particle function is approached with increasing interaction strength. The characteristic function is an extension of the two-particle part of the underlying Hamiltonian and governs the stability of the solution at intermediate and strong coupling. To handle situations with singularities in two-particle Green functions, we developed a systematic general scheme of approximations for the generating thermodynamic potential by summing diagrams classified at the level of two-particle functions. We used the linked-cluster theorem for the parquet-type diagrams to derive the appropriate generating functional and the one-particle self-energy. From this very general scheme, already known approximations involving two-particle functions can be derived. The construction, however, enables one to go systematically beyond simple theories and to include more complex diagrams also with higher-order vertex functions, when necessary.

The intermediate coupling falls into the critical region of a two-particle pole caused by condensation of electron–hole (bound) pairs. We stressed that any reliable approximation in a two-particle critical region must contain vertex corrections qualitatively equivalent to those embodied in the parquet algebra. This conclusion is dictated by a Ward-like identity (20*a*) reflecting conservation of charge, i.e. any variation of the electrostatic energy can be caused only by a variation in the charge distribution.

In an effort to comply with the demand of full renormalization of two-particle functions near critical points we proposed a simplified parquet algebra, called dipole approximation. This theory, mathematically expressed by *ansatze* (22*a*) and (23*a*), sums self-consistently contributions to the parquet diagrams from two topologically inequivalent channels. It neglects non-singular contributions and keeps only leading-order potentially divergent diagrams from multiple scatterings of electrons and holes. This approximation, having already two-particle functions with the full momentum dependence as in the parquet algebra, possesses a generating functional in closed form and represents a thermodynamically consistent, conserving approximation. The dipole approximation is an asymptotic solution of the parquet diagrams in the critical region of the metal–insulator transition with condensation of electron–hole singlet and triplet pairs.

We applied the dipole approximation to the Hubbard model in an external magnetic field. We showed that it becomes asymptotically exact at half-filling when the fully polarized ferromagnet is approached. Perturbation theory below the critical magnetic field, at which the saturated ferromagnet becomes unstable, is singular at strong coupling, and only a theory with renormalized two-particle functions can deliver a reliable description. Vertex renormalizations of the dipole approximation destroy the mean-field antiferromagnetic order in $d = 1$ dimensions and produce the asymptotics known from the Bethe *ansatz* solution.

The ultimate aim of the proposed scheme is to describe the Mott–Hubbard metal-insulator transition at zero magnetic field. The two two-particle functions from the dipole approximation show singularity of the same order at this transition. Unlike the case for a non-zero magnetic field, no apparent perturbative or iterative scheme for solving the non-linear integral equations (22*c*) and (23*b*) seems imminent. The only feasible way to reach a solution seems to be to factorize the leading divergent contribution via a low-frequency *ansatz* that would turn integral Bethe–Salpeter equations algebraic. However, a proper low-frequency *ansatz* leading to a consistent solution of the dipole or the parquet approximation appears rather complex. Work on the character of the two-particle singularity in the dipole approximation for the mean-field Hubbard and single-impurity Anderson model, from which the low-frequency *ansatz* must be deduced, is in progress.

Acknowledgment

This work was supported in part by grant No 202/95/0008 of the Grant Agency of the Czech Republic.

References

[1] Hubbard J 1964 *Proc. R. Soc.* A **281** 401
Brinkman W F and Rice T M 1970 *Phys. Rev.* B **2** 4302
[2] Georges A, Kotliar G, Krauth W and Rozenberg M 1996 *Rev. Mod. Phys.* **68** 13
[3] Jarrell M 1992 *Phys. Rev. Lett.* **69** 168
[4] Rozenberg M J, Zhang X Y and Kotliar G 1992 *Phys. Rev. Lett.* **69** 1236
[5] Georges A and Krauth W 1992 *Phys. Rev. Lett.* **69** 1240
[6] Ulmke M, Janiš V and Vollhardt D 1995 *Phys. Rev.* B **51** 10 411
[7] Georges A and Kotliar G 1992 *Phys. Rev.* B **45** 6479
[8] Zhang X Y, Rozenberg M J and Kotliar G 1993 *Phys. Rev. Lett.* **70** 1666
[9] Georges A and Krauth W 1993 *Phys. Rev.* B **48** 7167
[10] Rozenberg M J, Kotliar G and Zhang X Y 1994 *Phys. Rev.* B **49** 10 181
[11] Moeller G, Si Q, Kotliar G, Rozenberg M J and Fisher D S 1995 *Phys. Rev. Lett.* **74** 2082
[12] Dichtel K, Jelitto R J and Koppe H 1971 *Z. Phys.* B **246** 248
Jelitto R J 1973 *Z. Phys.* B **258** 175
[13] Hirsch J E 1990 *J. Appl. Phys.* **67** 4549
[14] Li Q P and Joynt R 1993 *Phys. Rev.* B **47** 3979
Li Q P and Joynt R 1994 *Phys. Rev.* B **49** 1632
[15] van Dongen P G J and Janiš V 1994 *Phys. Rev. Lett.* **72** 3258
[16] Baym G and Kadanoff L P 1961 *Phys. Rev.* **124** 287
[17] Baym G 1962 *Phys. Rev.* **127** 1391
[18] Janiš V and Schlipf J 1995 *Phys. Rev.* B **52** 17 119
[19] Weiner R A 1970 *Phys. Rev. Lett.* **24** 1071
Weiner R A 1971 *Phys. Rev.* B **4** 3165
[20] Jackson A D, Lande A and Smith R A 1982 *Phys. Rep.* **86** 55
[21] Menge B and Müller-Hartmann E 1991 *Z. Phys.* B **82** 237
[22] Suhl H 1967 *Phys. Rev. Lett.* **19** 442
[23] Bickers N E, Scalapino D J and White S R 1989 *Phys. Rev. Lett.* **62** 961
Bickers N E and Scalapino D J 1989 *Ann. Phys., NY* **193** 206
[24] Wortis M 1974 *Phase Transitions and Critical Phenomena* vol 3, ed C Domb and M S Green (London: Academic) p 121, equation (8)
[25] Wortis M, Jasnow D and Moore M A 1969 *Phys. Rev.* **185** 805
[26] Levine M and Suhl H 1968 *Phys. Rev.* **171** 567
Note that here the violation of charge conservation (20) is referred to as non-conservation of spin.
[27] Béal-Monod M T and Mills D L 1970 *Phys. Rev. Lett.* **24** 225
[28] Takahashi M 1969 *Prog. Theor. Phys.* **42** 1098